

Document Version

Final published version

Licence

CC BY

Citation (APA)

Fenski, M., Viezzer, D., Nguyen, V. A., Hufnagel, S., Grassow, L., Božić-Iven, M., Weingärtner, S., Kolbitsch, C., & Schulz-Menger, J. (2025). Evaluating the Effect of Heart Rate on T2 Balanced Steady-State Free Precession Cardiac MRI Mapping. *Radiology: Cardiothoracic Imaging*, 7(2), Article e240181. <https://doi.org/10.1148/ryct.240181>

Important note

To cite this publication, please use the final published version (if applicable).
Please check the document version above.

Copyright

In case the licence states “Dutch Copyright Act (Article 25fa)”, this publication was made available Green Open Access via the TU Delft Institutional Repository pursuant to Dutch Copyright Act (Article 25fa, the Taverne amendment). This provision does not affect copyright ownership.
Unless copyright is transferred by contract or statute, it remains with the copyright holder.

Sharing and reuse

Other than for strictly personal use, it is not permitted to download, forward or distribute the text or part of it, without the consent of the author(s) and/or copyright holder(s), unless the work is under an open content license such as Creative Commons.

Takedown policy

Please contact us and provide details if you believe this document breaches copyrights.
We will remove access to the work immediately and investigate your claim.

Evaluating the Effect of Heart Rate on T2 Balanced Steady-State Free Precession Cardiac MRI Mapping

Maximilian Fenski, MD^{1,2,3,4} • Darian Viezzer, MSc^{2,3,4,6} • Vy-An Nguyen^{2,3,4,6} • Simone Hufnagel, PhD⁵ • Leonard Grassow^{2,3,4} • Maša Božić-Iven, MSc^{7,8} • Sebastian Weingärtner, PhD⁷ • Christoph Kolbitsch, PhD⁵ • Jeanette Schulz-Menger, MD^{1,2,3,4,6}

Author affiliations, funding, and conflicts of interest are listed at the end of this article.

Radiology: Cardiothoracic Imaging 2025; 7(2):e240181 • <https://doi.org/10.1148/ryct.240181> • Content codes:  

Purpose: To evaluate heart rate as a patient-related confounder in a commonly applied T2 balanced steady-state free precession (bSSFP) mapping sequence used for myocardial tissue characterization.

Materials and Methods: This retrospective analysis included prospectively (from December 2013 to November 2021) acquired cardiac MRI (1.5 T) datasets with T2 bSSFP mapping from 69 healthy volunteers. Phantom studies and Bloch simulations were performed with heart rates of 60–130 beats per minute and different resting periods (three, six, or nine R-R intervals). Sequence parameters (repetition time, echo time, flip angle, echo train length) were matched across volunteer, phantom, and simulation measurements. Reference values covered clinically relevant T1 and T2 properties found in native myocardium (short, 1041 and 44 msec; medium, 1293 and 43 msec; long, 1534 and 40 msec). A mixed linear model assessed the effect of heart rate on T2 values in volunteer measurements.

Results: The study included 69 healthy volunteers (median age, 34 years; 44 female and 25 male). Heart rate influenced T2 values acquired with three R-R resting periods ($r = -0.38$, $P = .002$; linear regression slope, -0.7 msec/10 beats per minute [95% CI: -1.2 , -0.1]). In simulation and phantom measurements, T2 values acquired with three R-R resting periods strongly correlated with heart rate, irrespective of myocardial T1 and T2 properties ($r \leq -0.88$; $P < .01$ for all measurements). Heart rate dependency was reduced with increased resting periods in simulations and phantom measurements. Short myocardial T1 and T2 values derived from T2 bSSFP with nine R-R resting periods were not dependent on heart rate ($r = -0.41$; $P = .33$).

Conclusion: T2 bSSFP with three R-R resting periods underestimates T2 values with increasing heart rates. Use of longer resting periods with T2 bSSFP mapping sequences reduced heart rate dependency.

Supplemental material is available for this article.

Published under a CC BY 4.0 license.

Parametric mapping techniques are approaches for quantitative myocardial tissue characterization (1). A cardiac MRI examination, including T1 and T2 mapping, has been recommended in the workup of patients with suspected acute myocarditis (2,3). To differentiate between healthy and diseased tissue, T1 and T2 values should be compared with local reference ranges, and potential confounders should be considered (1). Both methodologic (4,5) and patient-related confounding factors (6–8) have been described in the literature.

For T1 mapping techniques, heart rate dependency is a well-known confounder (9,10), and considerable efforts have been made to understand and mitigate the underlying mechanisms (11–14). However, heart rate sensitivity with T2 mapping techniques is not as well studied. Recently, Hanson and colleagues (15) conducted a pooled analysis (46 studies, 954 healthy adults) to determine the extent of variability among parametric mapping-derived T2 values in healthy adults and to identify confounders. While they could not include heart rate in their model because it was not reported in any of the studies (15), a recent study showed significantly reduced T2 values with an increase in heart rate (16).

Commonly used T2 maps are generated from multiple single-shot T2-weighted images (17). These images are acquired using a T2 preparation module to induce different T2 sensitivity, followed by a fast readout sequence, such as balanced steady-state free precession (bSSFP) (18). Each source image

is acquired in a single heartbeat. The wait time between source images, also known as resting periods, is commonly defined in heartbeats (eg, three R-R intervals). Consequently, higher heart rates shorten the wait time between images, which may influence estimated T2 relaxation times.

The aim of this study was to examine the heart rate dependence of a commonly used T2 bSSFP sequence with three, six, and nine heartbeat resting periods using an analysis of healthy volunteer data, a phantom study, and Bloch simulations.

Materials and Methods

This study combines retrospective analysis of prospectively acquired data from healthy volunteers with phantom experiments and Bloch simulations. The study complied with the Declaration of Helsinki and was approved by the institutional ethics committee (study identification no. EA 1253 21). All participants provided written informed consent.

Healthy Volunteer Study

To create a dataset with T2 bSSFP mapping in healthy volunteers, a retrospective review of cardiac MRI studies that prospectively enrolled healthy adult volunteers and were performed at one tertiary center was carried out. The study included four completed investigations (19–22) with examinations performed between December 12, 2013, and November 8, 2021, and one ongoing study. All 70 cardiac MRI datasets

Abbreviations

bSSFP = balanced steady-state free precession, ICC = intraclass correlation coefficient

Summary

A T2 balanced steady-state free precession cardiac MRI mapping sequence with three R-R intervals underestimated myocardial T2 values as heart rate increased, but this dependence was mitigated by using longer resting periods.

Key Points

- T2 values acquired with T2 balanced steady-state free precession (bSSFP) and three R-R resting periods decreased with increasing heart rate in healthy participant and phantom measurements, with a slope between -0.63 and -0.79 msec/10 beats per minute ($P < .01$ for all measurements).
- Short myocardial T1 and T2 values derived from T2 bSSFP with nine R-R resting periods were not dependent on heart rate ($r = -0.41$; $P = .33$).
- A relevant threshold of 82 beats per minute was identified, above which the impact of heart rate with T2 bSSFP sequences with three R-R resting periods exceeds the intrareader variability.

Keywords

Cardiac, Phantom Studies, Myocardium, MRI, Confounding Variables

with T2 bSSFP mapping from a total of 70 volunteers collected in these studies were included in the present study. The participants were recruited for the control group or as traveling volunteers in a multicenter comparative study. Participants were excluded if they had known vascular, cardiac, or systemic conditions or any contraindications for cardiac MRI. All participants maintained sinus rhythm. A 12-lead electrocardiographic examination was performed to screen for conduction irregularities. Volunteer scans included at least one midventricular T2 short-axis section acquired in end diastole. Data from 68 of the 70 participants have already been published ($n = 17$ [19], $n = 17$ [20], $n = 21$ [21], $n = 12$ [22]). The data corresponding to the two participants included in the ongoing study have so far not been published. In comparison to the present study, none of the previous studies assessed heart rate as a confounder in T2 mapping techniques.

Imaging Protocol and Analysis

Cardiac MRI studies were performed using a 1.5-T scanner (Magnetom AvantoFit; Siemens Healthineers) at one medical center. A T2-prepared mapping sequence (19) with a bSSFP readout and identical imaging parameters was used for all simulations and scans (Table 1). Nonrigid motion correction was applied to avoid spatial misregistration of the source images. A two-parameter fitting model was used to generate the final T2 map.

Segmentation of Volunteer Images

Image analysis was performed by a single operator with 5 years of experience with cardiac MRI (M.F.) in consensus with a second operator (J.S.M., >25 years of experience) using CVI42 software (version 5.13.7; Circle Cardiovascular Imaging). The quality of the parametric maps was approved by visual assessment of each T2-weighted source and final mapping image. Only images that allowed clear delineation of the myocardium and surrounding

Table 1: Sequence Parameters of T2 bSSFP

Parameter	T2 bSSFP
Magnetization preparation	T2 preparation (0, 25, 55 msec)
Readout	bSSFP
Voxel sizing (mm)	1.6 × 1.6
TR (msec)	3.1
TE (msec)	1.15
Flip angle (degree)	70
Section thickness (mm)	6.0
FOV (mm)	270 × 360
Parallel imaging	GRAPPA
Acceleration factor	2
Bandwidth (Hz/pixel)	970

Note.—bSSFP = balanced steady-state free precession, FOV = field of view, GRAPPA = generalized autocalibrating partial parallel acquisition, TE = echo time, TR = recovery time.

borders and had no artifacts and residual motion were included. Heart rate during image acquisition was exported from the Digital Imaging and Communications in Medicine information (ie, DICOM) for each individual source image. A mean heart rate for each final map was calculated. To minimize partial volume effects, a 5% endo- and epicardial contour offset was used (20). The midventricular myocardium on T2 maps was subdivided into three equal segments using the anterior right-ventricular–left-ventricular insertion point as a reference. Only T2 times derived from midventricular septal regions were included to avoid susceptibility artifacts (1). Basal and apical sections were disregarded to omit potential partial volume effects due to residual diastolic wall motion, thin myocardium, or positioning close to the left ventricular outflow tract (21).

Relevant Heart Rate Threshold for Healthy Volunteers

A linear regression was used to describe the effect of heart rate on T2 values in volunteers. Heart rate dependence was defined as clinically relevant if its influence on T2 values exceeded the difference between two evaluations of the same reader (22). All volunteer images were therefore contoured by the same reader (M.F.) on two occasions at least 3 months apart, and the interval within which 95% of differences between two measurements by the same reader are expected to lie (95% limits of agreement) was calculated using a Bland-Altman plot. The value at which the influence of the heart rate exceeded the intrareader difference for our volunteer dataset was calculated as:

$$\text{Heart rate cutoff} = \frac{\text{lower 95\% bld altman limit}}{\text{slope linear regression}} + \text{median heart rate in HV}.$$

In addition, to allow for comparison with an interreader comparison-based approach, all volunteer images were contoured by a second reader (L.G.), and the lower 95% Bland-Altman limit of agreement between the two readers was calculated.

Bloch Simulations

The T2 mapping sequence described above was numerically simulated based on Bloch equations using MATLAB (R2022a;

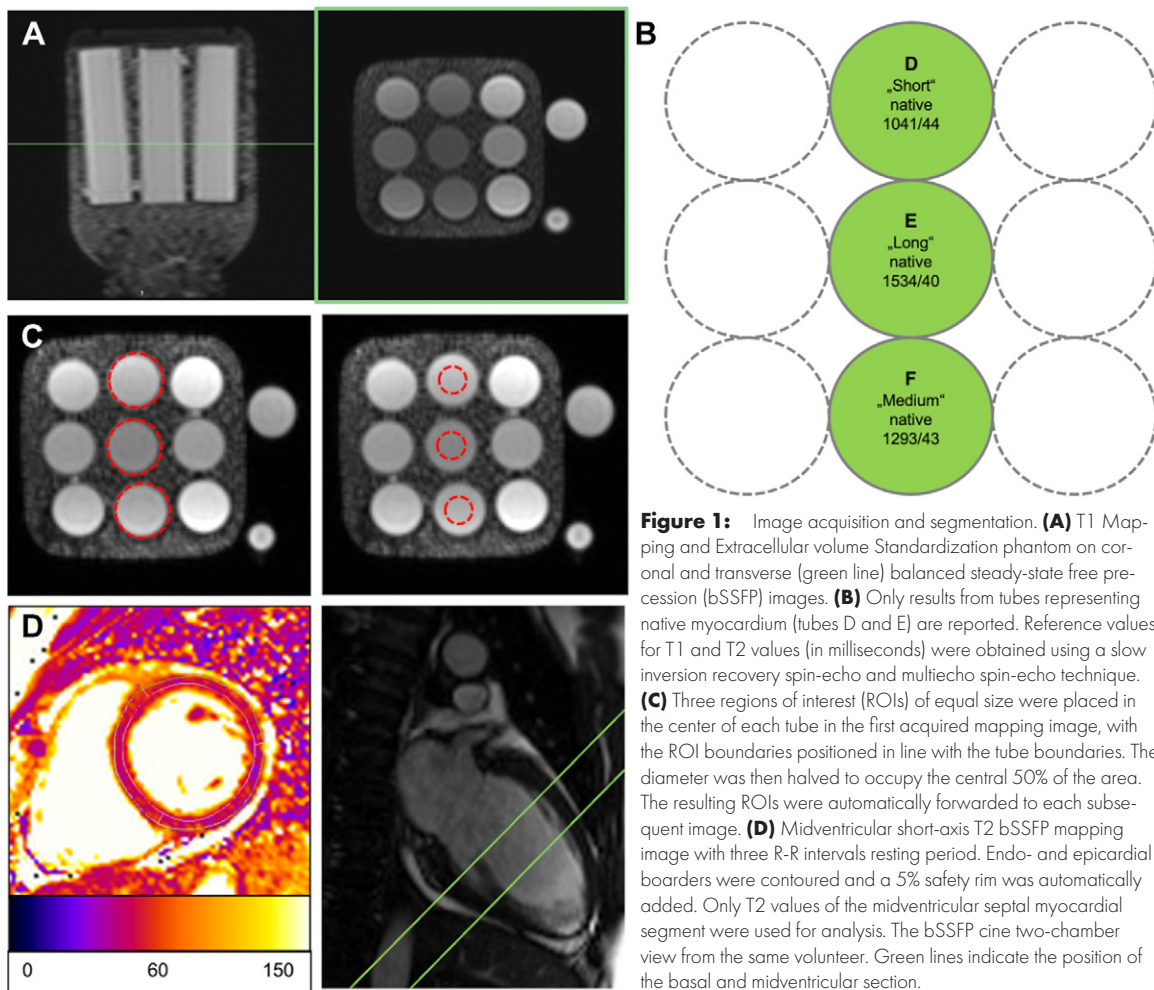


Figure 1: Image acquisition and segmentation. **(A)** T1 Mapping and Extracellular volume Standardization phantom on coronal and transverse (green line) balanced steady-state free precession (bSSFP) images. **(B)** Only results from tubes representing native myocardium (tubes D and E) are reported. Reference values for T1 and T2 values (in milliseconds) were obtained using a slow inversion recovery spin-echo and multiecho spin-echo technique. **(C)** Three regions of interest (ROIs) of equal size were placed in the center of each tube in the first acquired mapping image, with the ROI boundaries positioned in line with the tube boundaries. The diameter was then halved to occupy the central 50% of the area. The resulting ROIs were automatically forwarded to each subsequent image. **(D)** Midventricular short-axis T2 bSSFP mapping image with three R-R intervals resting period. Endo- and epicardial borders were contoured and a 5% safety rim was automatically added. Only T2 values of the midventricular septal myocardial segment were used for analysis. The bSSFP cine two-chamber view from the same volunteer. Green lines indicate the position of the basal and midventricular section.

MathWorks) with heart rates between 50 and 130 beats per minute and resting periods of three, six, and nine R-R intervals.

Phantom Study

The T1 Mapping and Extracellular volume Standardization (TIMES) program phantom was used, which covers clinically relevant ranges of T1 and T2 values in blood and myocardium (23). Parametric maps were consecutively acquired at regular heart rates between 60 and 130 beats per minute with increments of 10 beats per minute. Between each increment, measurements were separated by 10-second pauses to ensure sufficient longitudinal magnetization recovery. The whole protocol was repeated after the last image was acquired at 130 beats per minute. For electrocardiography simulation, an external commercial device was used (ES-300; S.P.L. Elektronik). The reference T1 value was measured by an inversion recovery prepared spin-echo sequence with a repetition time of 8 seconds; an echo time of 12 msec; and inversion times of 25, 50, 300, 600, 2400, or 4800 msec. The reference T2 value was measured by a spin echo sequence with a repetition time of 3000 seconds and echo time of 24, 50, 100, 200, 300, or 400 msec.

Segmentation of Phantom Images

A self-developed Python-based tool was used to ensure equal region of interest sizing and positioning according to published

methods (4). Regions of interest of equal size were manually placed in the first acquired mapping image and aligned with the tube boundaries. The diameter was then halved to avoid any partial volume effects with the surrounding material (Fig 1). These regions of interest were automatically transferred to each subsequent mapping image.

Statistical Analysis

All data were analyzed using SPSS software (version 28.0; SPSS) and MATLAB (version R2021b; MathWorks). The distribution of the parameters was assessed using the Shapiro-Wilk test and Q-Q plots. Continuous variables are reported as means \pm SDs or medians \pm IQRs. For phantom measurements, correlation analysis between T2 values and heart rate was performed using the Spearman test and linear regression analysis. To evaluate the effects of different factors on T2 values in volunteers, a mixed linear model with backward selection and without a random effect was used. The following fixed factors were included: age, sex, and heart rate. Visual assessment of the linear regression assumptions was performed by examining scatterplots of residuals versus fitted values for linearity and homoscedasticity, a Q-Q plot for normality, and correlation matrices for multicollinearity (if appropriate). Comparisons between two groups were made using an independent *t* test or the Mann-Whitney test for continuous vari-

ables. A χ^2 test was performed for noncontinuous variables. Cases with missing data were excluded from the analysis. A two-tailed α less than .05 was considered statistically significant. As this is an exploratory study, no adjustments for multiple comparisons were made.

To assess intrareader differences, all volunteer images and a subset of phantom images were contoured twice by the same

reader (M.F.). For interreader comparison, a second reader (L.G.) contoured all volunteer datasets. The readers were blinded to prior measurement results. Bland-Altman plots and the intraclass correlation coefficient (ICC) were used to evaluate bias and reliability.

Results

Participant Characteristics

A total of 70 scans meeting the inclusion criteria were identified, with participants recruited between December 2013 and November 2021. Figure 2 provides a flow diagram outlining the screening process. One dataset was excluded due to artifacts caused by B0 field inhomogeneities from a fluid-filled stomach. The final dataset comprised 69 volunteers (median age, 34 years [IQR, 28–49]), including 44 female and 25 male participants. Baseline characteristics are summarized in Table 2. Female participants were significantly older than male participants (median age, 38 years [IQR, 30–52] vs 29 years [IQR, 24–36]; $P = .004$).

Volunteer Study

A total of 69 midventricular T2 mapping images were acquired. Of 69 septal segments, four segments (5.8%) were excluded due to artifacts. T2 relaxation times per section and mean heart rate during source image acquisition are shown in Table 3. Mean T2 values were $51.1 \text{ msec} \pm 2.3$. Heart rate (median, 68 beats per minute [IQR, 63–77]; minimum, 51 beats per minute; maximum, 101 beats per minute) was significantly correlated with T2 values at Spearman analysis ($r_s = 0.38$ [95% CI: -0.56 ,

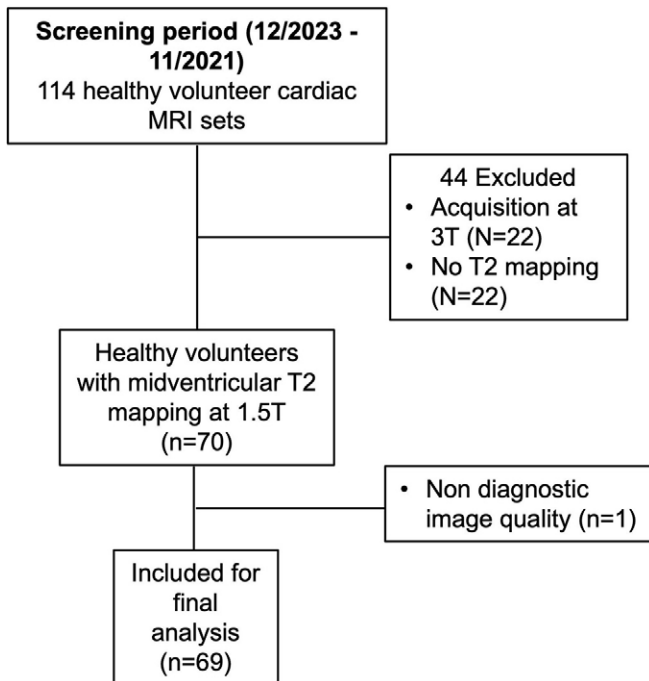


Figure 2: Flowchart outlines the screening process.

Table 2: Baseline Characteristics of Healthy Volunteers

Parameter	Overall (n = 69)	Male Participants (n = 25)	Female Participants (n = 44)	P Value*
Age (y)	34 (28–49)	29 (24–36)	38 (30–52)	.004
Height (cm)	173.3 ± 8.3	179.4 ± 8.4	169.8 ± 5.9	<.001
Weight (kg)	69.2 ± 9.7	73.4 ± 10.6	66.7 ± 8.3	.005
BMI	23.0 ± 3.0	22.8 ± 2.8	23.2 ± 3.1	.97
Body surface area (m ²)	1.8 ± 0.2	1.9 ± 0.2	1.8 ± 0.1	<.001
SBP (mm Hg)	121 ± 13	120 ± 11	121 ± 14	.78
DBP (mm Hg)	72 ± 8	70 ± 5	73 ± 9	.13
LV EDV (mL)	151 ± 29	169 ± 28	142 ± 24	<.001
LV EDV/BSA (mL/m ²)	83.2 ± 14.4	88.8 ± 14.5	80.1 ± 13.6	.02
LV EDV/H (mL/cm)	0.86 ± 0.18	0.91 ± 0.24	0.83 ± 0.14	.10
LV SV (mL)	94 ± 17	101 ± 18	90 ± 16	.004
LV SV/BSA (mL/m ²)	51.6 ± 8.5	53.4 ± 8.8	50.6 ± 8.3	.20
LV EF (%)	62.3 ± 4.8	60.3 ± 4.5	63.4 ± 4.7	.009
LV mass (g)	91.7 ± 20.5	109.0 ± 20.7	82.3 ± 13.0	<.001
LV mass/BSA (g/m ²)	49.5 ± 11.3	54.8 ± 15.2	46.5 ± 7.0	.003
LV mass/H (g/cm)	0.52 ± 0.12	0.58 ± 0.16	0.49 ± 0.08	<.001

Note.—Unless otherwise noted, data are means ± SDs or medians with IQRs in parentheses. BMI = body mass index (calculated as weight in kilograms divided by height in meters squared), BSA = body surface area, DBP = diastolic blood pressure, EDV = end diastolic volume, EF = ejection fraction, H = height, LV = left ventricular, SBP = systolic blood pressure, SV = stroke volume. * Unpaired two-sided t test between male and female volunteers for normally distributed data, otherwise, a Mann-Whitney U test was used.

Table 3: Midventricular Septal T2 Times and Heart Rate during Source Image Acquisition in Healthy Volunteers

Parameter	All (<i>n</i> = 69)	Male Participants (<i>n</i> = 25)	Female Participants (<i>n</i> = 44)
Heart rate (beats/min)	68 (63–77)	67 (62–77)	71 (63–77)
T2 value (msec)	51.1 ± 2.3 (50.5, 51.7)	51.0 ± 2.6 (50.0, 52.0)	51.2 ± 2.2 (50.6, 51.9)

Note.—Data are displayed as means ± SDs with 95% CIs in parentheses or medians with IQRs in parentheses.

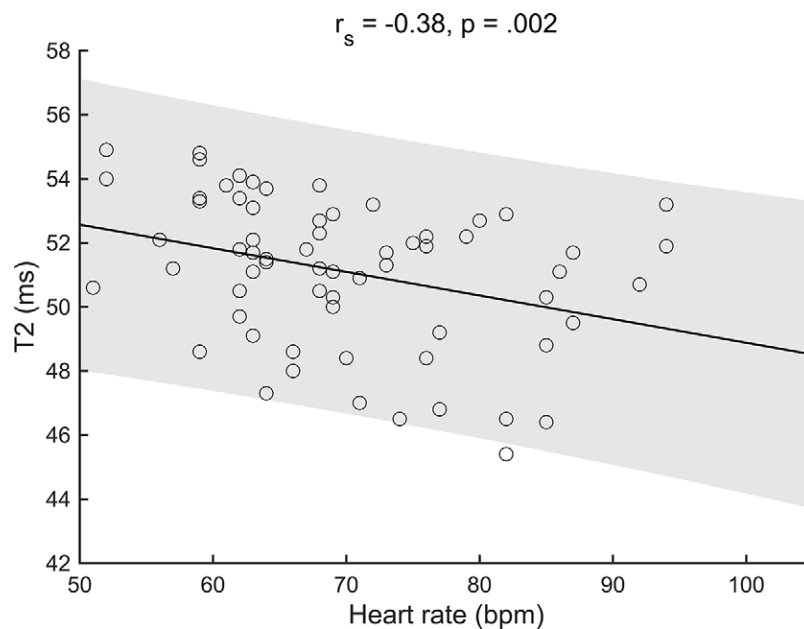


Figure 3: Correlation between heart rate and T2 times in 69 healthy volunteers. Dots represent each mean septal midventricular myocardial T2 value. The consistent line represents the linear regression line between T2 values and heart rate. The gray area indicates the 95% CI of the regression line. bpm = beats per minute, r_s = Spearman correlation coefficient.

–0.09]; $P = .002$) (Fig 3), as well as in the multiple linear regression model (standardized β , –0.276 [95% CI: –0.112, –0.003]; $P = .04$). With multiple linear regression analysis, T2 values decreased with increased heart rate, with a slope of –0.7 msec/10 beats per minute (95% CI: –1.2, –0.1). Neither sex nor age was associated with T2 measurements. The detailed results of the mixed model and individual regression analysis can be found in Appendix S1.

Bloch Simulations

In simulation studies, T2 values obtained with three, six, and nine R-R rest periods showed a negative correlation with heart rate over the entire simulated range ($r = -1$; $P < .05$ for all measurements). However, the slopes were considerably less steep with increasing resting periods as shown in Figure 4.

Phantom Study

All 48 final T2 mapping images could be used for analysis. T2 values measured with three R-R resting periods showed a decrease with higher heart rates in all phantom tubes representing native myocardial T1 and T2 properties ($r = -1$; $P < .01$ for all measurements) (Fig 5). Table 4 shows the slopes of the

regression equations expressing the relationship between heart rate and T2 values. The dependence on heart rate decreased with increasing resting periods. T2 bSSFP with nine R-R intervals showed the least sensitivity to heart rate (nine R-R: $r = -0.41$ [95% CI: –0.87, 0.44]; $P = .32$ for short myocardial T1 and T2 values), and the six R-R variant demonstrated no effect of heart rate on T2 values for heart rates from 60 to 90 beats per minute (60 beats per minute: 53.53 msec; 90 beats per minute: 53.48 msec).

Due to the flow properties of blood, which cannot be represented by the phantom, the results of tubes A–C (representing blood T1 and T2 properties) are not reported. Furthermore, the results of tubes G–I (representing myocardial T1 and T2 properties after contrast material application) are not reported as the evaluated sequence was not designed to sample the faster T1 and T2 recovery curves in these scenarios. The results for every tube and heart rate can be found in Appendix S1 along with the detailed results of the correlation analysis.

Intra- and Interreader Comparison

ICC analysis showed excellent intra- and interreader reliability for the volunteer measurements (intrareader ICC, 0.97 [95%

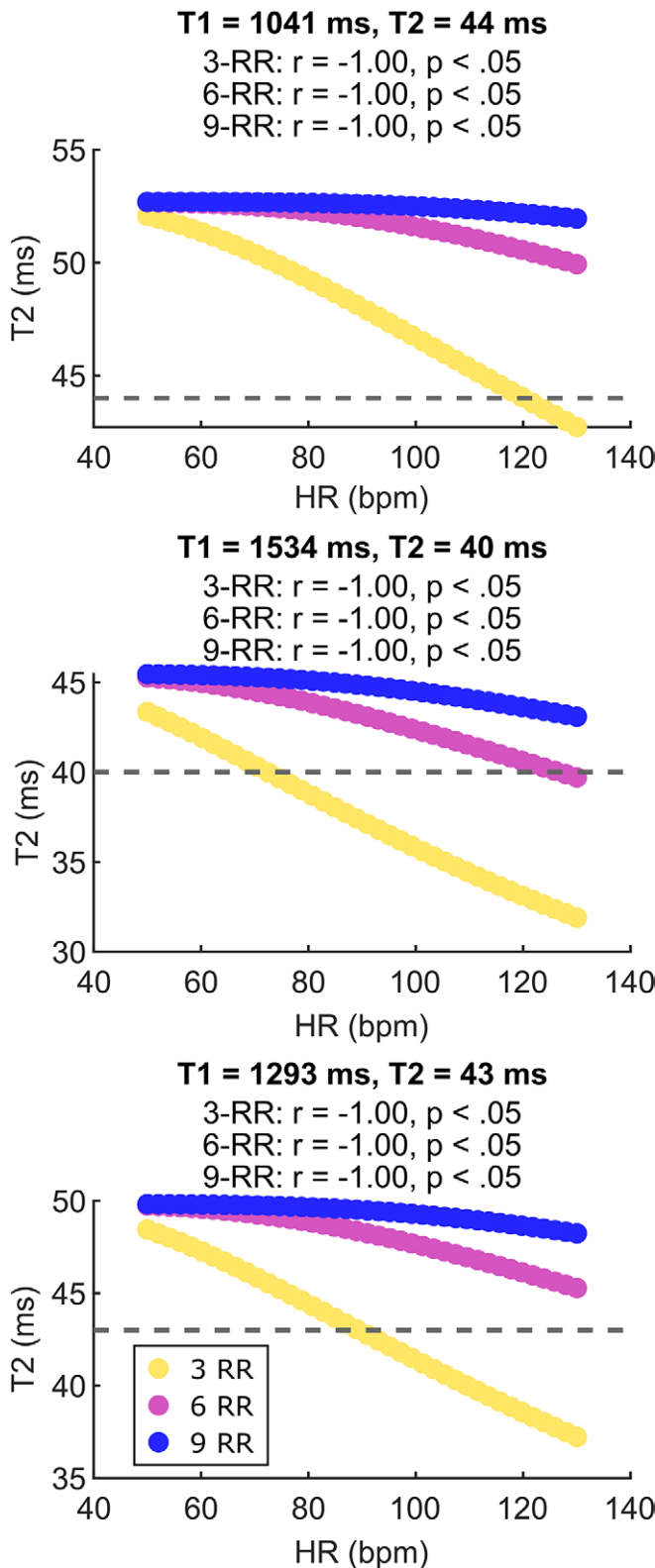


Figure 4: Bloch simulations with different resting periods (three, six, and nine R-R intervals) and different T1 and T2 values representing native short-to-long myocardial properties. Dotted line indicates the true T2 value. Simulated sequence parameters (repetition time, time to echo, flip angle, echo train length) were matched with phantom and healthy volunteer measurements. bpm = beats per minute, HR = heart rate.

CI: 0.96, 0.98]; interreader ICC, 0.94 [95% CI: 0.91, 0.96]), and Bland-Altman analysis showed no relevant intrareader or interreader bias (intrareader bias, 0.13 msec; interreader bias,

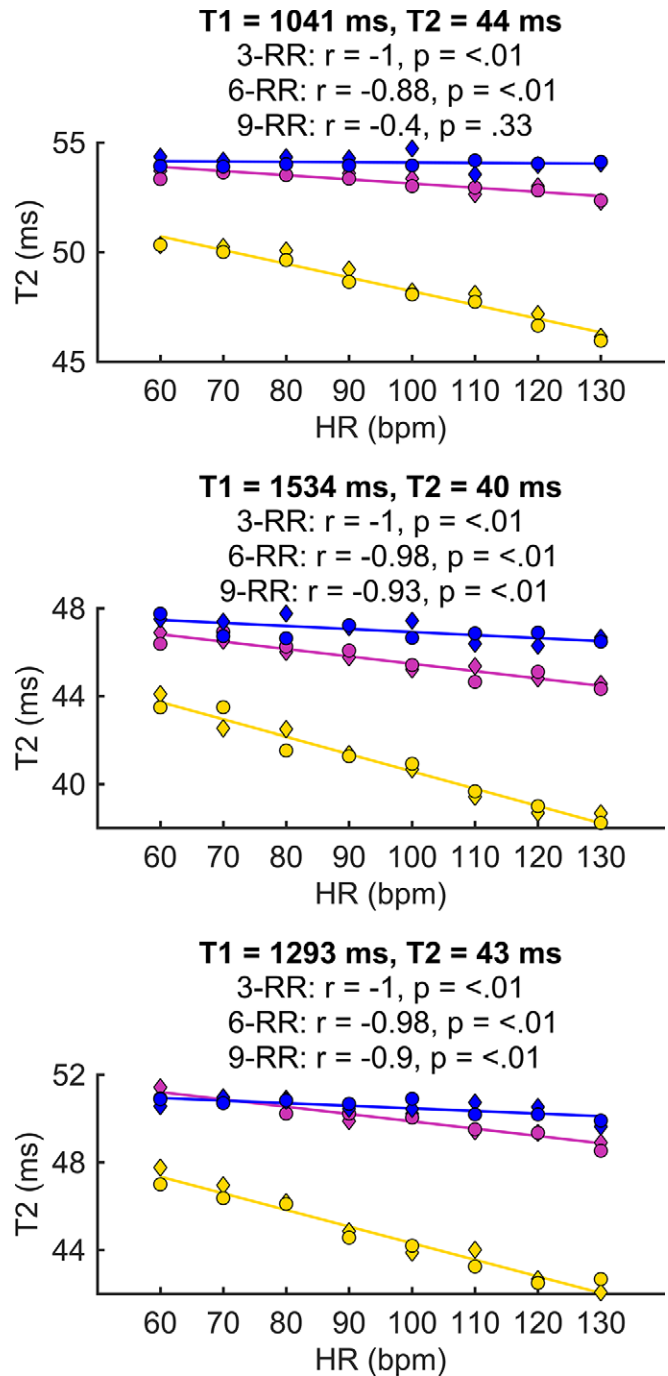


Figure 5: Phantom measurements. Correlation between heart rate and T2 values (in milliseconds) in a T1 and T2 range representing native myocardial properties. T2 balanced steady-state free precession with three (yellow), six (pink), and nine (blue) R-R resting periods. The diamonds represent the first measurement, the dots represent the second measurement, and the consistent line represents the regression line for the mean value between the first and second measurement. bpm = beats per minute, HR = heart rate, r = Spearman correlation coefficient.

0.02 msec). Furthermore, there was excellent reliability and no bias between two readings for the phantom measurements. A detailed intrareader analysis can be found in Appendix S1.

Clinically Relevant Heart Rate Threshold

The 95% limits of agreement for the intra- and interreader comparison were -0.96 to 1.2 msec and -1.5 to 1.4 msec,

Table 4: Slopes of the Linear Regression Equations Expressing the Relationship between Heart Rate and Measured T2 Times based on Phantom Measurements

Tube Name (T1 and T2)	T2 bSSFP Three R-R	T2 bSSFP Six R-R	T2 bSSFP Nine R-R
D (1041 and 44 msec)	-0.63 (-0.74, -0.52)	-0.19 (-0.28, -0.10)	-0.02* (-0.07, 0.04)
E (1534 and 40 msec)	-0.79 (-0.86, -0.71)	-0.36 (-0.40, -0.27)	-0.14 (-0.20, -0.08)
F (1293 and 43 msec)	-0.76 (-0.86, -0.65)	-0.33 (-0.39, -0.27)	-0.12 (-0.20, -0.04)

Note.—Values are given as slope (in milliseconds)/10 beats per minute with 95% CIs in parentheses. bSSFP = balanced steady-state free precession.

* Correlation coefficient not significant ($P > .05$).

respectively. A correlation between T2 values and heart rate could be found in our volunteer study with a slope of -0.07 msec/beats per minute. The median heart rate was 68 beats per minute. The relevant cutoff at which the influence of heart rate exceeded the intraobserver and interobserver variability was therefore calculated as 82 beats per minute and 89 beats per minute, respectively.

Discussion

The present study investigated the influence of heart rate on a commonly used T2 bSSFP mapping sequence with different resting periods using Bloch simulations, a phantom study, and an analysis of data from 69 healthy volunteers. The main findings are that T2 bSSFP with a resting period of three R-R intervals significantly underestimates T2 values with increasing heart rates, and that the heart rate dependence can be mitigated by using longer resting periods. In the phantom study, a heart rate–dependent underestimation of -0.63 msec/10 beats per minute was found in a tissue with T1 and T2 properties of 1041 and 44 msec. Matching this, midventricular T2 times in healthy volunteers measured with T2 bSSFP with a resting period of three R-R intervals decreased with heart rate with a slope of -0.7 msec/10 beats per minute. Furthermore, in our cohort with a median heart rate of 68 beats per minute, influence of heart rate on T2 measurements exceeded the intrareader variability at 82 beats per minute and interreader variability at 89 beats per minute.

In our *in silico* and phantom study, the factors that influenced heart rate dependency were the number of resting periods and the T1 properties of the underlying tissue. To produce quantitative maps of myocardial T2 relaxation times, multiple images of varying T2 sensitivity are acquired over multiple cardiac cycles (19). The signal intensities across these T2-weighted source images are then fitted to a decay equation to generate the final T2 map (18). To allow the magnetization to return to its equilibrium state between preparation pulses, a resting period is implemented. This waiting time is often defined in heartbeats. Higher heart rates therefore shorten the waiting time between images, which can introduce T1 weighting into the signal due to incomplete T1 magnetization recovery (18). Depending on the order of the preparation times, this leads to an underestimation (short-to-long preparation times) or an overestimation (long-to-short

preparation times) of the T2 times. Most commonly, T2 mapping is performed with increasing preparation times, resulting in heart rate–dependent underestimation. This mechanism can be mitigated by using longer resting periods which allow the magnetization to return to its equilibrium state, even at higher heart rates. In addition, tissues with long T1 properties require more time to return to equilibrium, which was reflected in our phantom measurements in steeper regression curves in tissues with longer T1 properties.

The mean midventricular T2 times in our volunteer study was $51.1 \text{ msec} \pm 2.3$, which aligns well with the pooled mean of 52 msec at 1.5 T (95% CI: 51, 53) in a recent meta-analysis that included 42 studies (15). In contrast to the studies by Bönner et al (7) and Thomas et al (16), we did not find a sex- or age-specific difference in T2 values. While it is possible that our findings may have been influenced by a type II error, they are consistent with a recent meta-analysis of 954 healthy adults that found no association between myocardial T2 times with age or sex (15). We indicated a significant decrease in midventricular T2 times with increasing heart rates with a slope of -0.7 msec/10 beats per minute. This is in concordance with previous studies, which showed significantly reduced T2 values with an increase in heart rate (8,24). Another recent study identified a significant association between T2 values, derived from T2-preparation bSSFP mapping and heart rate (16). The authors reported a slope of -0.74 msec/10 beats per minute, which aligns closely with our observed slope. In contrast, no heart rate dependence was found in a study reporting normal T2 values obtained in 100 healthy volunteers by using a multiecho fast spin-echo sequence with four echo times (25). However, the authors did not report the number of resting periods. Therefore, results may not be comparable to our volunteer study if longer resting periods were used. To allow comparison between T2 mapping studies, the reporting of the number of recovery periods should be considered in future studies involving T2 mapping techniques. This is especially true given that T2 values in our simulation and phantom study differed between three, six, and nine R-R resting periods even at 60 beats per minute, indicating relevant differences between these variants even at lower heart rates.

The clinical relevance of our findings must be evaluated in the context of the practical application of T2 values and the precision required in clinical assessments. To distinguish health from disease, T2 values should be compared with local reference

ranges, taking potential confounders into account (1). The normal myocardial T2 range is commonly defined as the mean \pm 2 SDs of the local reference cohort, and the diagnosis of myocardial edema would be made if T2 values exceeded this range within an appropriate clinical context. Given that heart rate can vary substantially among individuals, a patient with a heart rate deviating by, for example, 30 beats per minute from the average could experience a change in T2 time of approximately 2.1 msec. This alteration could shift the T2 value within the normal range, even though elevated T2 values would be present. The second scenario where the influence of heart rate should be considered is in the sequential monitoring of T2 values, such as in evaluating the impact of an intervention on T2 values. Variations in heart rate could account for observed differences, rather than the intervention or the disease progression itself. Appendix S1 provides recommendations for mitigating heart rate dependency, a detailed discussion of additional factors affecting the reproducibility of T2 mapping results, and a brief outlook into recent developments of T2 mapping sequences. It also includes a discussion of the discrepancy between reference T2 values and those derived from T2 bSSFP sequences.

This study had several limitations. First, nonrigid motion correction was used in our study to avoid spatial misregistration of the source images. However, we did not evaluate the effect of motion correction methods on measured T1 and T2 values. Second, in our phantom study, we utilized simulated heart rates ranging from 60 to 130 beats per minute and demonstrated an inverse linear relationship between heart rate and measured T2 values for T2 bSSFP with three R-R resting periods. Nevertheless, it is possible that a plateau effect may be seen at even lower heart rates, which was not illustrated in this study. Furthermore, due to the lower sampling rate of T2 values at both very low and very high heart rates in our volunteer study, any assertion regarding the influence of heart rate on T2 values in these marginal areas is subject to greater uncertainty. Further studies with a larger sample size are therefore needed to validate our results. Third, as this is an exploratory study, no adjustments for multiple comparisons were made and this may have introduced a type I error. Fourth, we compared the influence of heart rate with intrareader and interreader variability. However, interstudy variability, which accounts for the impact of B0 shimming and other operator-dependent tasks on T2 measurements, was not assessed in our study. Fifth, we investigated the effect of age, sex, and heart rate on T2 values. However, we did not include ethnicity in our model. Dedicated future studies are needed to determine whether ethnicity-specific T1 and T2 mapping reference values are warranted. Last, we indicate a perfect inverse correlation between heart rate and measured T2 values in Bloch simulations and phantom experiments. These observations were made under simulation or laboratory conditions. Under real-world conditions, more confounders are to be expected, and the occurrence of a perfect correlation is therefore very unlikely.

In conclusion, our study demonstrated that T2 bSSFP with three R-R intervals underestimates T2 values with increasing heart rates. Acquisition schemes with longer or fixed resting periods (ie, \geq six R-R intervals) may be used to mitigate T2 underestimation with higher heart rates. Future research should investigate the sensitivity of T2 bSSFP sequences with a fixed recovery period

(eg, 3 seconds) to variations in heart rate and arrhythmias. Additionally, future studies should explore whether newer techniques, such as MR fingerprinting–based T2 sequences, can address heart rate and arrhythmia dependencies.

Author affiliations:

¹ Department of Cardiology and Nephrology, Helios Klinikum Berlin Buch, Berlin, Germany

² Experimental and Clinical Research Center, a cooperation between the Max Delbrück Center for Molecular Medicine in the Helmholtz Association and Charité Universitätsmedizin Berlin, Berlin, Germany

³ Experimental and Clinical Research Center, Charité–Universitätsmedizin Berlin, corporate member of Freie Universität Berlin and Humboldt-Universität zu Berlin, Lindenberger Weg 80, 13125 Berlin, Germany

⁴ Max Delbrück Center for Molecular Medicine in the Helmholtz Association (MDC), Berlin, Germany

⁵ Physikalisch-Technische Bundesanstalt (PTB), Braunschweig and Berlin, Germany

⁶ German Center for Cardiovascular Research (DZHK), Partner Site Berlin, Berlin, Germany

⁷ Department of Imaging Physics, Delft University of Technology, Delft, the Netherlands

⁸ Medical Faculty Mannheim, Heidelberg University, Mannheim, Germany

Received May 20, 2024; revision requested June 14; revision received January 10, 2025; accepted January 31.

Address correspondence to: J.S.M. (email: jeanette.schulz-menger@charite.de).

Funding: M.F. receives funding from the German Heart Foundation (S/09/23). D.V. acknowledges funding by the German Center for Cardiovascular Research (DZHK). The working group led by J.S.M. holds research grants from Siemens Healthineers. None of the funding entities interfered or influenced the research.

Author contributions: Guarantors of integrity of entire study, M.F., J.S.M.; study concepts/study design or data acquisition or data analysis/interpretation, all authors; manuscript drafting or manuscript revision for important intellectual content, all authors; approval of final version of submitted manuscript, all authors; agrees to ensure any questions related to the work are appropriately resolved, all authors; literature research, M.F., V.A.N., J.S.M.; clinical studies, M.F., L.G., J.S.M.; experimental studies, M.F., V.A.N., S.H., M.B.I., S.W., C.K., J.S.M.; statistical analysis, M.F., D.V., S.H., M.B.I.; and manuscript editing, M.F., D.V., S.H., L.G., M.B.I., C.K., J.S.M.

Data sharing: Data generated or analyzed during the study are available from the corresponding author by reasonable request.

Disclosures of conflicts of interest: M.F. No relevant relationships. D.V. No relevant relationships. V.A.N. No relevant relationships. S.H. Funding from the German Research Foundation, BIOQIC. L.G. No relevant relationships. M.B.I. Scholarship through the Landesgraduiertenförderung Baden-Württemberg. S.W. Grants from the European Research Council (grant no. 101078711), Nederlandse Hartstichting (grant no. 03-004-2022-0079), the 4TU Precision Medicine program supported by High Tech for a Sustainable Future TU Delft, Erasmus MC Convergence Impulse Award ZonMw (grant no. 04510011910073), and 4TU.Federation, a Dutch Research Council Nederlandse Organisatie voor Wetenschappelijk Onderzoek (NWO) Start-up grant STU.019.024, ZonMw. C.K. No relevant relationships. J.S.M. No relevant relationships.

References

- Messroghli DR, Moon JC, Ferreira VM, et al. Clinical recommendations for cardiovascular magnetic resonance mapping of T1, T2, T2* and extracellular volume: A consensus statement by the Society for Cardiovascular Magnetic Resonance (SCMR) endorsed by the European Association for Cardiovascular Imaging (EACVI). *J Cardiovasc Magn Reson* 2017;19(1):75. [Published correction appears in *J Cardiovasc Magn Reson* 2018;20(1):9.]
- McDonagh TA, Metra M, Adamo M, et al. 2021 ESC Guidelines for the diagnosis and treatment of acute and chronic heart failure. *Eur Heart J* 2021;42(36):3599–3726.
- Ferreira VM, Schulz-Menger J, Holmvang G, et al. Cardiovascular Magnetic Resonance in Nonischemic Myocardial Inflammation: Expert Recommendations. *J Am Coll Cardiol* 2018;72(24):3158–3176.
- Captur G, Bhandari A, Brühl R, et al. T₁ mapping performance and measurement repeatability: results from the multi-national T₁ mapping standardization phantom program (T1MES). *J Cardiovasc Magn Reson* 2020;22(1):31.
- Baefler B, Schaarschmidt F, Stehning C, Schnackenburg B, Maintz D, Bunck AC. A systematic evaluation of three different cardiac T2-mapping sequences at 1.5 and 3T in healthy volunteers. *Eur J Radiol* 2015;84(11):2161–2170.

6. Piechnik SK, Ferreira VM, Lewandowski AJ, et al. Normal variation of magnetic resonance T1 relaxation times in the human population at 1.5 T using ShMOLLI. *J Cardiovasc Magn Reson* 2013;15(1):13.
7. Bönner F, Janzarik N, Jacoby C, et al. Myocardial T2 mapping reveals age- and sex-related differences in volunteers. *J Cardiovasc Magn Reson* 2015;17(1):9.
8. von Knobelsdorff-Brenkenhoff F, Prothmann M, Dieringer MA, et al. Myocardial T1 and T2 mapping at 3 T: reference values, influencing factors and implications. *J Cardiovasc Magn Reson* 2013;15(1):53.
9. Kellman P, Hansen MS. T1-mapping in the heart: accuracy and precision. *J Cardiovasc Magn Reson* 2014;16(1):2.
10. Xu Z, Li W, Wang J, et al. Reference ranges of myocardial T1 and T2 mapping in healthy Chinese adults: a multicenter 3T cardiovascular magnetic resonance study. *J Cardiovasc Magn Reson* 2023;25(1):64.
11. Fitts M, Breton E, Kholmovski EG, et al. Arrhythmia insensitive rapid cardiac T1 mapping pulse sequence. *Magn Reson Med* 2013;70(5):1274–1282.
12. Xue H, Greiser A, Zuehlsdorff S, et al. Phase-sensitive inversion recovery for myocardial T1 mapping with motion correction and parametric fitting. *Magn Reson Med* 2013;69(5):1408–1420.
13. Piechnik SK, Ferreira VM, Dall'Armellina E, et al. Shortened Modified Look-Locker Inversion recovery (ShMOLLI) for clinical myocardial T1-mapping at 1.5 and 3 T within a 9 heartbeat breathhold. *J Cardiovasc Magn Reson* 2010;12(1):69.
14. Weingärtner S, Akçakaya M, Basha T, et al. Combined saturation/inversion recovery sequences for improved evaluation of scar and diffuse fibrosis in patients with arrhythmia or heart rate variability. *Magn Reson Med* 2014;71(3):1024–1034.
15. Hanson CA, Kamath A, Gottbrecht M, Ibrahim S, Salerno M. T2 Relaxation Times at Cardiac MRI in Healthy Adults: A Systematic Review and Meta-Analysis. *Radiology* 2020;297(2):344–351.
16. Thomas KE, Lukaszuk E, Shanmuganathan M, et al. Misclassification of females and males in cardiovascular magnetic resonance parametric mapping: the importance of sex-specific normal ranges for diagnosis of health vs. disease. *Eur Heart J Cardiovasc Imaging* 2024;25(3):339–346.
17. Huang TY, Liu YJ, Stemmer A, Poncelet BP. T2 measurement of the human myocardium using a T2-prepared transient-state TrueFISP sequence. *Magn Reson Med* 2007;57(5):960–966.
18. O'Brien AT, Gil KE, Varghese J, Simonetti OP, Zareba KM. T2 mapping in myocardial disease: a comprehensive review. *J Cardiovasc Magn Reson* 2022;24(1):33.
19. Giri S, Chung YC, Merchant A, et al. T2 quantification for improved detection of myocardial edema. *J Cardiovasc Magn Reson* 2009;11(1):56.
20. Schulz-Menger J, Bluemke DA, Bremerich J, et al. Standardized image interpretation and post-processing in cardiovascular magnetic resonance - 2020 update: Society for Cardiovascular Magnetic Resonance (SCMR): Board of Trustees Task Force on Standardized Post-Processing. *J Cardiovasc Magn Reson* 2020;22(1):19.
21. Wassmuth R, Prothmann M, Utz W, et al. Variability and homogeneity of cardiovascular magnetic resonance myocardial T2-mapping in volunteers compared to patients with edema. *J Cardiovasc Magn Reson* 2013;15(1):27.
22. Zange L, Muehlberg F, Blaszczyk E, et al. Quantification in cardiovascular magnetic resonance: agreement of software from three different vendors on assessment of left ventricular function, 2D flow and parametric mapping. *J Cardiovasc Magn Reson* 2019;21(1):12.
23. Captur G, Gatehouse P, Keenan KE, et al. A medical device-grade T1 and ECV phantom for global T1 mapping quality assurance-the T₁ Mapping and ECV Standardization in cardiovascular magnetic resonance (T1MES) program. *J Cardiovasc Magn Reson* 2016;18(1):58.
24. Thavendiranathan P, Walls M, Giri S, et al. Improved detection of myocardial involvement in acute inflammatory cardiomyopathies using T2 mapping. *Circ Cardiovasc Imaging* 2012;5(1):102–110.
25. Meloni A, Nicola M, Positano V, et al. Myocardial T2 values at 1.5 T by a segmental approach with healthy aging and gender. *Eur Radiol* 2022;32(5):2962–2975.